Complete Landing Autopilot having Control Laws Based on Neural Networks and Dynamic Inversion

Mihai Lungu, Romulus Lungu
University of Craiova, Faculty of Electrical Engineering, Craiova, Romania
Lma1312@yahoo.com, romulus_lungu@yahoo.com

***Abstract*—This paper discusses the automatic control of airplane in longitudinal and lateral-directional planes, during landing, using two neural network and dynamic inversion concept based adaptive control subsystems, having as components: linear observers, linear dynamic compensators, reference models, and Pseudo Control Hedging blocks in order to eliminate the adapting difficulties of the neural network appearing because of the actuators' nonlinearities. Two subsystems (for longitudinal and lateral-directional planes) will be put together and a new complete landing auto-pilot will result; it is software implemented the results' accuracy and the achievement of the precision standards being briefly analyzed.**

Keywords— landing; airplane; neural network; dynamic inversion

I. INTRODUCTION

Landing is a very difficult flight stage; airplanes have to perform precise maneuvers near the ground to land in safely conditions, at desired touch points with satisfactory sink rate, attitude, and speed. There are difficulties to land safely, with conventional controllers, because atmospheric conditions and the airplanes' dynamics change drastically during all the flight and landing phases. The precise knowledge of the controllable system's mathematical model is needed in order to design perfect conventional controllers. Moreover, the altitude and flight conditions modify the airplane dynamics, and, therefore, the adaptive controllers are excelent choices [1]. The feedback linearization (one of most used nonlinear control technique) is employed in [2] to control the landing procedure; unfortunately, the feedback linearization method presents a disadvantage with respect to the necessity to have in the same equation all the plant uncertainties [3]. Other automatic landing system (ALS) has been designed in [4] using a back-propagation learning algorithm based feed-forward neural networks, the main disadvantage being related to the need of a priori training on normal and faulty operating data. The presence of known nonlinearities associated to the dynamics of airplane or actuators as well as to the external disturbances motivates the need of adaptive control architectures consisting of neural networks and Pseudo Control Hedging blocks [5, 6]. The main advantages of the dynamic inversion are: 1) plant nonlinearities are cancelled; 2) closed loop plants behave like stable linear systems; 3) simplicity of the control, global exponential stability of the tracking error, and ease of implementation. The strong point of the neural networks (NNs) is their approximation ability and their capacity to approximate the dynamics of an unknown system through learning. Taking into account all the advantages of the NNs, dynamic inversion approach, Pseudo Control Hedging blocks and the combining of these elements with state observers, linear dynamic compensators, and blocks modelling the geometry of landing, the paper brings novelty in the research area of ALSs' design. Also, the main weakness of the papers dealing with landing is that the automatic landing systems have been designed for the longitudinal plane or for the lateral-directional one. The present paper focuses on airplane's automatic control in the two planes using the neural networks and dynamic inversion based control techniques. Our purpose is to design and validate a new ALS (both planes) cancelling the negative effect of possible disturbances (errors of the sensors, crosswind, or wind shears). The paper is a combination of the works [1] and [3]; each of them treats only one plane, while in the current paper a complete ALS is obtained.

II. AIRPLANE CONTROL IN LONGITUDINAL PLANE

During landing, there can be distinguished three main stages: initial approach, glide slope, and flare [7]. The initial approach is equivalent with the airplane's descent from the cruise altitude to approximately 420 m above the ground for heavy airplane or less (light airplane) – the phase in lateral-directional plane. During next two stages, both in longitudinal plane, the speed and the altitude must be controlled; these two stages are: 1) ***Glide slope phase*** ($H \geq H_0$) and 2) ***Flare phase*** ($H < H_0$); H is the airplane altitude, while H_0 is the altitude from which the flare starts. The equations describing the airplane's landing geometry in longitudinal (vertical) plane are [8]: $X_{p_0} = X_p - H_p / \tan(\gamma_c)$ and

$$H_c = \begin{cases} (X - X_{p_0}) \cdot \tan(\gamma_c), H \geq H_0, \\ H_c = H_0 \exp((X_0 - X)/\tau \dot{X}) \Leftrightarrow \dot{H}_c = -H_c / \tau, H < H_0, \end{cases} \quad (1)$$

where X is the horizontal coordinate associated to the airplane displacement, $\tau -$ the time constant defining the exponential curve associated to flare: $V_0 \tau = 0.9741 (X - X_{p_0})$; $A_p (X_p, H_p)$ is the starting point for the glide slope phase, $V_0 -$ airplane nominal velocity. For longitudinal plane, it is proved in [1] that the geometry of airplane motion is described by the equation: $\dot{X} = V_x \cos\theta + V_z \sin\theta, V_z = V_0 \sin\alpha,$ where V_x and V_z are the airplane speed components along its longitudinal and normal axes, $\theta -$ the pitch angle, while α is the attack angle.

The new landing subsystem for longitudinal plane contains: 1) a subsystem for calculation of the variable H_c; 2) reference models; 3) dynamic inversion and neural network based adaptive controller; 4) a PCH block which makes the system work in the nonlinearities' linear zones. The reference models are used for obtaining the calculated altitude and the desired flight velocity.

978-1-5090-4862-5/17/$31.00 ©2017 IEEE

The first automatic landing subsystem contains an adaptive system for the control of the output vector $y=[H\ V_x]^T$. The structure of the adaptive control subsystem (fig. 1) has on its direct way of the closed loop having unitary feedback an adaptive controller and a system (A+ACT) consisting of the nonlinear model (having the function h_r) and the reduced order linear model (having the transfer matrix $H_d(s)$). The control law $\hat{v}$ may be chosen of the following form [1, 9]:

$$\hat{v}=v_{pd}+\hat{v}_r-v_a+\bar{v}, \tag{2}$$

where the signal v_{pd} (output of a linear dynamic compensator) is used for the stabilization of airplane linear dynamics, v_a – an adaptive component (output of a neural network – NN_c) is useful to compensate the nonlinear function $h_r(v,y)$ approximation error (ε), functions interfering in the airplane and actuators' dynamics, $\hat{v}_r$ (signal provided by the reference models) is used to cancel the system's deviation $\tilde{y}$ and its derivatives, while $\bar{v}$ is a robustness component. The state of the longitudinal dynamics is $\boldsymbol{x}=[V_x\ \alpha\ \omega_y\ \theta\ H]^T$ [1]; $\omega_y=\dot{\theta}$ is the pitch rate. The command vector of the first subsystem is chosen as: $u=[\delta_p\ \delta_T]^T$, where δ_p is the elevator deflection and δ_T – the thrust command; their equations are:

$$T_p\dot{\delta}_p+\delta_p=\delta_{p_c},T_T\dot{\delta}_T+\delta_T=\delta_{T_c}, \tag{3}$$

with δ_{p_c} and δ_{T_c} – the commands applied to elevator and to engines, respectively; T_p and T_T are time constants. If the servo-elevator is described by a nonlinear dynamics, the first equation (3) is replaced by the model from fig. 2 (with $\hat{v}_i=\hat{v}_1,\delta_i=\delta_p$, $T_i=T_p,v_{h_i}=v_{h_1}$). Because, the adaptive controllers are sensitive to actuators' nonlinearities, in these controllers' architectures, one should introduce Pseudo Control Hedging (PCH) blocks which limit the signal v by means of a component representing the estimation of the actuators' dynamics. The output signal of the PCH block (v_{h_1}) is a reference model's additional input.

The ensemble airplane-actuators (A+ACT) is described by equation [10]: $\dot{\boldsymbol{x}}=A_v\boldsymbol{x}+B_vu$, with $\boldsymbol{x}=[V_x\ \alpha\ \omega_y\ \theta\ H\ \delta_p\ \delta_T]^T$, $u=[\delta_{p_c}\ \delta_{T_c}]^T$; the expressions of A_v and B_v are presented in [1]. The system A+ACT is generally described by state equations: $\dot{\boldsymbol{x}}=f(\boldsymbol{x},u),y=h(\boldsymbol{x})$, with f and h – generally unknown nonlinear/linear functions, calculated in the linearization process with realtion to the landing trajectory.

The relative degrees of the system with respect to the variables y_i are denoted with $r_i,i=\overline{1,2};r=r_1+r_2$ is the relative degree of the system with respect to the output vector. The control law $\hat{v}=\hat{h}_r(y,\hat{u})$ represents the best approximation of the function $v=h_r(y,u)$; the approximation error of the function $h_r(y,u)$ is $\varepsilon=[\varepsilon_1\ \varepsilon_2]^T$ having the following form: $\varepsilon=h_r(y,u)-\hat{h}_r(y,\hat{u})$. In [1] one has obtained $r_1=3,r_2=2$,

$$r=5,\begin{bmatrix}\dddot{H}+\ddot{H}\\ \ddot{V}_x\end{bmatrix}=\begin{bmatrix}c_1 & c_2 & c_3 & c_4 & 0 & c_p & c_t\\ d_1 & d_2 & d_3 & d_4 & 0 & d_p & d_t\end{bmatrix}\boldsymbol{x}+\begin{bmatrix}\frac{a_{52}b_{21}}{T_p} & 0\\ 0 & \frac{b_{12}}{T_T}\end{bmatrix}\begin{bmatrix}\delta_{p_c}\\ \delta_{T_c}\end{bmatrix};$$

it can be written: $y^{(r)}=-\lambda^TY+v,v=\hat{v}+\varepsilon$, with $\lambda=[\lambda_1\ \lambda_2]^T$, $Y=[Y_1\ Y_2]^T,h_r=[h_{r_1}\ h_{r_2}]^T$. By identification, one gets [1]:

$$\hat{u}=\begin{bmatrix}\hat{\delta}_{p_c}\\ \hat{\delta}_{T_c}\end{bmatrix}=\hat{h}_r^{-1}(y,\hat{v})=\begin{bmatrix}\frac{a_{52}b_{21}}{T_p} & 0\\ 0 & \frac{b_{12}}{T_T}\end{bmatrix}^{-1}\left\{\hat{v}-\begin{bmatrix}c_1\\ d_1\end{bmatrix}V_x\right\}, \tag{4}$$

with $\hat{v}=\begin{bmatrix}\hat{v}_1\\ \hat{v}_2\end{bmatrix},\varepsilon=\begin{bmatrix}\varepsilon_1\\ \varepsilon_2\end{bmatrix}=\begin{bmatrix}c_2 & c_3 & c_4 & c_p & c_t\\ d_2 & d_3 & d_4 & d_p & d_t\end{bmatrix}[\alpha\ \omega_y\ \theta\ \delta_p\ \delta_T]^T$.
Using the expressions for reduced order linear subsystems' transfer functions, one uses the reference models for y_1 and y_2; the block diagrams of the blocks modelling these reference models are presented in Fig. 3. Beside $\bar{y}_i$, the reference models provide the components $\hat{v}_{r_i},i=\overline{1,2}$, of the vector $\hat{v}_r=[\hat{v}_{r_1}\ \hat{v}_{r_2}]^T$. This vector is obtained from the condition that the vector y and its derivatives tend to their imposed values, i.e. $y^{(r)}=\bar{y}^{(r)}$ and $Y=\bar{Y}$, which is obtained in steady regime when $v_a=\varepsilon$ and $v=\hat{v}$; this means that the approximation error is compensated by the adaptive component; from equation $y^{(r)}=-\lambda^TY+v$, $v=\hat{v}$, one obtains: $\hat{v}_r=\bar{y}^{(r)}+\lambda^T\bar{Y}$, with $\lambda=[\lambda_1\ \lambda_2]^T=$ $=[0\ 0\ 1\ 0\ 0]^T$. Thus, $\hat{v}_{r_1}=\dddot{\bar{y}}_1+\ddot{\bar{y}}_1$ and $\hat{v}_{r_2}=\ddot{\bar{y}}_2$. Moreover, from (4), omitting the term which contains δ_{T_c}, one gets: $\hat{v}_1=c_1V_x+\frac{a_{52}b_{21}}{T_p}\hat{\delta}_{p_c},\hat{\delta}_{p_c}=\frac{T_p}{a_{52}b_{21}}(\hat{v}_1-c_1V_x)$. By substituting $\hat{v}_1$ with $\bar{v}_1$ and $\hat{\delta}_{p_c}$ with $\bar{\delta}_p$ in the previous equation and $\hat{\delta}_{p_c}$ with δ_{p_c}, the functions $\hat{h}_{r_1}$ and $\hat{h}_{r_1}^{-1}$ from fig. 2 are deduced [1]:

$$\bar{v}_1=c_1V_x+\frac{a_{52}b_{21}}{T_p}\bar{\delta}_p,\delta_{p_c}=\hat{h}_{r_1}^{-1}(y,\hat{v}_1)=\frac{T_p}{a_{52}b_{21}}(\bar{v}_1-c_1V_x). \tag{5}$$

The two components of the vector v_{pd} (the output of the dynamic compensator) are: $v_{pd_1}=k_{p_1}\tilde{y}_1+k_{d_1}\dot{\tilde{y}}_1=[k_{p_1}\ k_{d_1}\ 0]\cdot$

$\cdot[\tilde{y}_1\ \dot{\tilde{y}}_1\ \ddot{\tilde{y}}_1]^T=d_{c_1}\boldsymbol{e}_1,v_{pd_2}=k_{p_2}\tilde{y}_2+k_{d_2}\dot{\tilde{y}}_2=[k_{p_2}\ k_{d_2}][\tilde{y}_2\ \dot{\tilde{y}}_2]^T=d_{c_2}\boldsymbol{e}_2$,
with $\boldsymbol{e}_1=[\tilde{y}_1\ \dot{\tilde{y}}_1\ \ddot{\tilde{y}}_1]^T$ – the vector of errors with respect to the state y_1 associated to the reduced order subsystem having $r_1=3$, while $\boldsymbol{e}_2=[\tilde{y}_2\ \dot{\tilde{y}}_2]^T$ – the error state vector of the system with respect to the state y_2 associated to the other reduced order subsystem $(r_2=2)$. The notations $d_{c_1}=[k_{p_1}\ k_{d_1}\ 0]$ and $d_{c_2}=[k_{p_2}\ k_{d_2}]$ are used; k_{p_i} and k_{d_i}, are the compensator's coefficients; with this method, one obtains the vector [1]:

$$v_{pd} = \begin{bmatrix} v_{pd_1} \\ v_{pd_2} \end{bmatrix} = \begin{bmatrix} d_{c_1}\boldsymbol{e}_1 & d_{c_2}\boldsymbol{e}_2 \end{bmatrix}^T = \begin{bmatrix} d_{c_1} & 0_{1\times 2} \\ 0_{1\times 3} & d_{c_2} \end{bmatrix} \begin{bmatrix} \boldsymbol{e}_1 \\ \boldsymbol{e}_2 \end{bmatrix} = D_c \boldsymbol{e}.$$

The linear observer estimates the state vector $\boldsymbol{e}$ providing $\hat{\boldsymbol{e}}$ (estimation of the vector $\boldsymbol{e}$); the observer uses only the input vector: $z_c = \tilde{y} = \begin{bmatrix} \tilde{y}_1 & \tilde{y}_2 \end{bmatrix}^T = \begin{bmatrix} c_1\boldsymbol{e}_1 & c_2\boldsymbol{e}_2 \end{bmatrix}^T = \begin{bmatrix} c_1 & 0 \\ 0 & c_2 \end{bmatrix} \boldsymbol{e} = \overline{C}\boldsymbol{e}$, with $C = \begin{bmatrix} c_1 & 0_{1\times 3} \\ 0_{1\times 2} & c_2 \end{bmatrix}$, $c_1 = \begin{bmatrix} 1 & 0 & 0 \end{bmatrix}, c_2 = \begin{bmatrix} 1 & 0 \end{bmatrix}$. The observer is modeled by the equations [1, 11]:

$$\dot{\hat{\boldsymbol{e}}} = \widetilde{A}\hat{\boldsymbol{e}} + L z_c, \widetilde{A} = \overline{A} - L\overline{C}, \tag{6}$$

where L is the observer's gain matrix which is calculated in order to obtain an asymptotically stable matrix $\widetilde{A}$. For the obtaining of the adaptive control law, one considers a feed-forward neural network (NN_c) consisting of 3 layers: an input layer (with n_1 neurons), a hidden layer (with n_2 neurons), and an output layer (with n_3 neurons); W denotes the matrix consisting of the weights associated to the links between the hidden layer's neurons and output layer's neurons and V – the matrix consisting of the weights associated to the links between the input layer neurons and the hidden layer neurons. The adaptive control law is [6]:

$$v_a = W^T \sigma\left(V^T \eta\right), \tag{7}$$

where the matrices W and V, associated to the NN_c's weights, are the solutions of the equations' system [12]:

$$\begin{cases} \dot{W} = -k_W \left[2\left(\sigma - \sigma' V^T \eta\right)\overline{\boldsymbol{e}} + k\left(W - W_0\right) \right], \\ \dot{V} = -k_V \left[2\eta \overline{\boldsymbol{e}} W^T \sigma' + k\left(V - V_0\right) \right], \end{cases} \tag{8}$$

with $\overline{\boldsymbol{e}} = \hat{\boldsymbol{e}}^T P\overline{B}; \sigma' = \left.\dfrac{\mathrm{d}\sigma}{\mathrm{dz}}\right|_{z=z_0}$ – Jacobian of the vectorial sigmoid function σ, k_W, k_V – positive constants; the expressions for obtaining k is presented in detail in [1]. The vector η is:

$$\eta = \begin{bmatrix} 1 & \hat{v}_d^T & y_d^T \end{bmatrix}^T = \begin{bmatrix} 1 & I_1 & I_2 & \ldots & I_{n1} \end{bmatrix}^T; \tag{9}$$

$\hat{v}_d^T = \left[\hat{v}(t)\ \hat{v}(t-d)\ \ldots\ \hat{v}\left(t-(n_1-r-2)d\right)\right]$, d – the sample step, $y_d^T = \left[y(t)\ y(t-d)\ \ldots\ y\left(t-(n_1-r-3)d\right)\right]$, while $I_i, i = \overline{1, n_1}$ are the neural network's outputs. The expression $\overline{v}$ (the robustness component of the control law (2)) is borrowed from [1] or [6]; the next equation is used:

$$\overline{v}^T = k_z \left(\left\| F \right\|_f + \overline{F} \right) \left\| \hat{\boldsymbol{e}} \right\| \frac{\overline{\boldsymbol{e}}}{\left\| \overline{\boldsymbol{e}} \right\|} + k_e \overline{\boldsymbol{e}}, \tag{10}$$

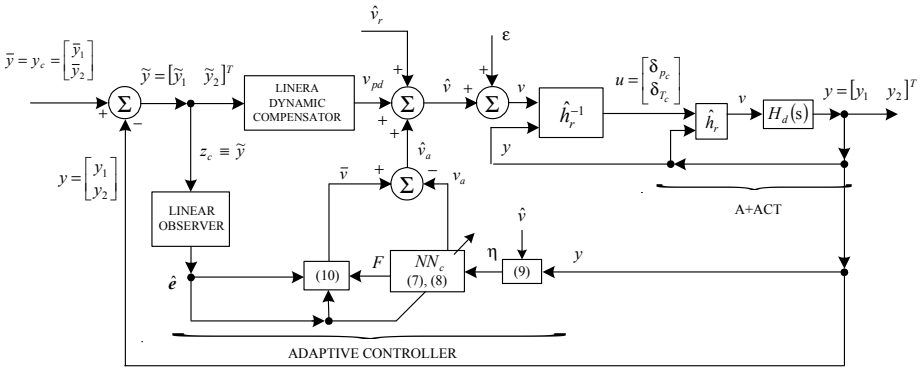

Fig. 1. The adaptive control subsystem of the output vector y

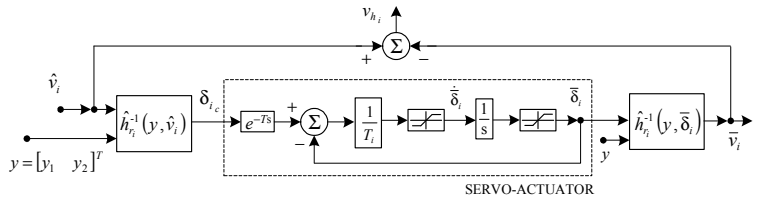

Fig. 2. Block diagram associated to the actuators and to the PCH blocks

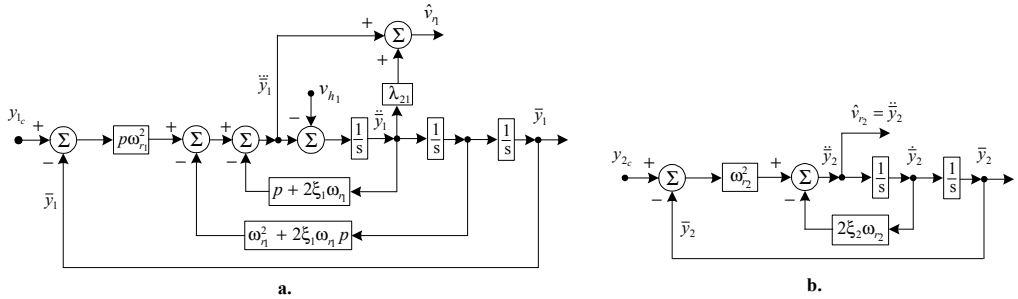

a. **b.**

Fig. 3. Block diagrams of the reference models: a) r_1=3 and b) r_2=2

with k_z and $k_e -$ positive gains, $F = \begin{bmatrix} W & 0 \\ 0 & V \end{bmatrix}; \|F\|_f^2 = \text{tr}\{F^T F\} \le \overline{F}; \|F\|_f$ is the Frobenius norm of the matrix F, while $\overline{F}$ is the neural network's ideal matrix. The role of the robustness component $\overline{v}$ is to ensure the boundedness of the neural network's matrices W and V.

III. Airplane Control in Lateral-Directional Plane and the Structure of the New ALS

For the in lateral-directional plane, the landing geometry is detailed in [3]; the second main subsystem of the new designed ALS must cancel airplane's lateral deviation relative to the runway; its main control subsystem is again the adaptive system presented in Fig. 1. The lateral dynamics associated state is $x = [V_y \ \omega_x \ \omega_z \ \varphi \ \Delta\psi]^T$ with $V_y -$ the airplane's lateral velocity, ω_x and $\omega_z -$ the roll and the yaw angular rates, $\varphi -$ the roll angle, $\Delta\psi -$ the variation of the flight direction angle; δ_e and δ_d are the actuators' states ($\delta_e -$ ailerons and $\delta_d -$ rudder's deflections). The linear equations of the actuators (servo-aileron and servo-rudder) are [3]:

$$T_e\dot{\delta}_e + \delta_e = \delta_{e_c}, T_d\dot{\delta}_d + \delta_d = \delta_{d_c}, \quad (11)$$

or the ones describing the nonlinear subsystems of the PCH models in Fig. 2; for $i = e, \delta_{i_c} = \delta_{e_c}$ is the command of the aileron's actuator, while, for $i = d, \delta_{i_c} = \delta_{d_c}$ is the command of the rudder associated actuator. For the system containing the lateral-directional dynamics and the actuators' linear or nonlinear dynamics is $u = [\delta_{e_c} \ \delta_{d_c}]^T$. By using the same procedure as in section II, the relative degrees r_1 and r_2 are obtained: $r_1 = r_2 = 3, r = 6$. One also obtains [3]:

$$\hat{u} = \begin{bmatrix} \hat{\delta}_{e_c} \\ \hat{\delta}_{d_c} \end{bmatrix} = \hat{h}_r^{-1}(y, \hat{v}) = \begin{bmatrix} \frac{b_{21}}{T_e} & \frac{b_{22}}{T_d} \\ \frac{b_{31}}{T_e} & \frac{b_{32}}{T_d} \end{bmatrix}^{-1} \left\{ \hat{v} - \begin{bmatrix} c_4 \\ d_4 \end{bmatrix} \varphi \right\}, \quad (12)$$

$$\varepsilon = \begin{bmatrix} \varepsilon_1 \\ \varepsilon_2 \end{bmatrix} = \begin{bmatrix} c_1 & c_2 & c_3 & c_e & c_d \\ d_1 & d_2 & d_3 & d_e & d_d \end{bmatrix} [V_y \ \omega_x \ \omega_z \ \delta_e \ \delta_d]^T. \quad (13)$$

The control law u has the form (12), where $\hat{v}$ is replaced with v and $\hat{\delta}$ with δ. The reference models are the ones in Fig. 3.a. The signals v_{h_i} from this figure are the components of the vector $v_h -$ the output of the PCH nonlinear consisting of two subsystems having the architectures in Fig. 2. The PCH block is introduced when the servo-aileron and servo-rudder are nonlinear, issue affecting the neural networks' functioning. Using again the above presented methodology, one also obtains: $\hat{v}_1 = c_4\varphi + \frac{b_{21}}{T_e}\hat{\delta}_{e_c}, \hat{v}_2 = d_4\varphi + \frac{b_{32}}{T_d}\hat{\delta}_{d_c}, \overline{v}_1 = \hat{h}_{r_1}(y, \overline{\delta}_1) = \hat{h}_{r_1}(y, \overline{\delta}_e) = c_4\varphi + \frac{b_{21}}{T_e}\overline{\delta}_e, \overline{v}_2 = \hat{h}_{r_2}(y, \overline{\delta}_2) = \hat{h}_{r_2}(y, \overline{\delta}_d) = d_4\varphi + \frac{b_{32}}{T_d}\overline{\delta}_d$. For the lateral-directional plane, the system in Fig. 1 has the state vector

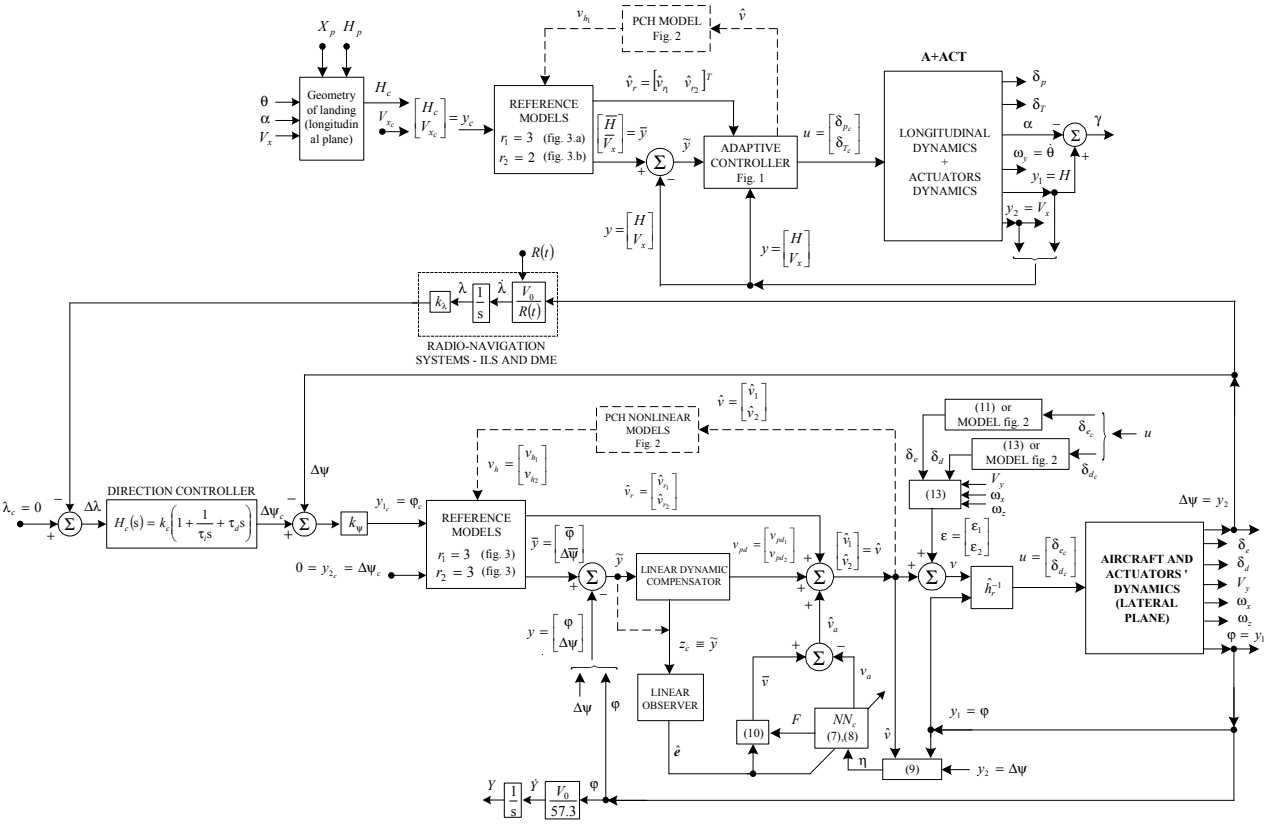

Fig. 4. New automatic landing system's block diagram (both planes)

$\boldsymbol{e}=\left[\tilde{y}\ \dot{\tilde{y}}\ \ddot{\tilde{y}}\right]^T=\left[e\ \dot{e}\ \ddot{e}\right]^T=\left[\tilde{y}_1\ \dot{\tilde{y}}_1\ \ddot{\tilde{y}}_1\ \tilde{y}_2\ \dot{\tilde{y}}_2\ \ddot{\tilde{y}}_2\right]^T$. If a PD linear dynamic compensator is chosen, its state is $\boldsymbol{e}=\left[e_1\ e_2\right]^T=$ $=\tilde{y}=\left[\tilde{y}_1\ \tilde{y}_2\right]^T=\left[\tilde{\varphi}\ \Delta\tilde{\psi}\right]^T$, with $\tilde{\varphi}=\bar{\varphi}-\varphi$ and $\Delta\tilde{\psi}=\Delta\bar{\psi}-\Delta\psi$. The expression of the control law v_{pd} is [3]:

$$v_{pd}=\left[d_{c_1}\boldsymbol{e}_1\ \ d_{c_2}\boldsymbol{e}_2\ \right]^T=D_c\left[\boldsymbol{e}_1\ \ \boldsymbol{e}_2\right]^T=\begin{bmatrix}k_{p_1} & k_{d_1} & 0 & 0 & 0 & 0\\ 0 & 0 & 0 & k_{p_2} & k_{d_2} & 0\end{bmatrix}\boldsymbol{e}. \quad (14)$$

Because in steady regime $\hat{v}=\varepsilon=v=0$, one obtains the the error model's equation: $\dot{\boldsymbol{e}}=A\boldsymbol{e}-Bv$, $v=v_{pd}+\hat{v}_r+\hat{v}_a+\varepsilon$, with $\boldsymbol{e}=\bar{Z}-Z=\left[\boldsymbol{e}_1\ \boldsymbol{e}_2\right]^T$. Replacing in previous equations $v_{pd}=D_c\boldsymbol{e}$, one gets: $\dot{\boldsymbol{e}}=\bar{A}\boldsymbol{e}-\bar{B}\left(\hat{v}_r+\hat{v}_a+\varepsilon\right),\hat{v}_a=\bar{v}-v_a,\bar{B}=B,$ $\bar{A}=A-BD_c$ [3]. The structure of the new neural network based ALS, using dynamic inversion, is presented in Fig. 4; it consists of two subsystems – one for longitudinal plane and one for the lateral-directional plane. For the first one, the airplane's speed (V_x) and altitude (H) are controlled in order to track the desired trajectory. In lateral plane, there are controlled the airplane's roll angle (φ) and the error angle $\Delta\psi=\bar{\psi}-\psi$ (difference between $\bar{\psi}-$ runway's direction and $\psi-$ airplane's flight direction).

IV. Numerical Simulation Results

To study the functionality of the new ALS, one considers a light airplane (Charlie type) [10]; the coefficients associated to its dynamics (both planes) are given in [1] and [3]. The reference models' coefficients have the following values: $p=0.5,\xi_1=0.7,$ $\omega_{n_1}=2.5\,\text{rad/s},\omega_{n_2}=2.5\,\text{rad/s},\xi_2=0.7,$ while the control limits of the servo-actuators are $\pm5\,\text{deg}$ and $\pm5\,\text{deg/s}$, respectively. For longitudinal plane, using the linear subsystems' characteristic equations (having unitary negative feedbacks) having the outputs $\bar{y}_1$ and $\bar{y}_2$, the values of the dynamic compensators' parameters are calculated; imposing for the characteristics equations $s^3+s^2+k_{d_1}s+k_{p_1}=0,s^2+k_{d_2}s+k_{p2}=0,$ the roots -0.1, -0.2, -0.3 and -1.1, -0.7, respectively, one gets: $k_{p_1}=0.02,$ $k_{d_1}=0.27,k_{p_2}=0.77,k_{d_2}=0.8.$ For lateral-directional plane, imposing for characteristics eqs. $s^3+s^2+k_{d_i}s+k_{p_i}=0,i=\overline{1,2},$ negative roots (e.g. -0.1, -0.2, -0.3 and -1.1, -0.7, -0.6), it results: $k_{p_1}=0.0193,k_{d_1}=0.27,k_{p_2}=0.77,k_{d_2}=0.8.$ The new ALS (Fig. 4) has been software implemented in Matlab/Simulink and one obtained the time characteristics for the glide slope (Fig. 5.a) and flare (Fig. 5.b); for lateral plane, one obtained the characteristics in Fig. 6. If the actuators are nonlinear, one uses a PCH block $(v_h\neq0)$ because these allow the system work in the nonlinearities' linear zones. For the longitudinal plane, the characteristics prove the new ALS's stability and small overshoots. There can be remarked some differences between the case "with PCH block" and "without PCH block". When the actuator is nonlinear, the PCH's usage does not modify the variables' final values, but the transient regime period decreases. One may remark in Fig. 5 that the slope angle is in accordance with its theoretical values: -2.5 deg for the glide slope and 0 deg for the flare. During glide slope, the airplane is characterized by a descending trajectory (4th graphic in Fig. 5.a), while the flare trajectory is a parabolic one (4th graphic in Fig. 5.b) with a null slope angle. Analyzing Fig. 5, one remarks that the altitude error is less than 0.5 m during glide slope and 0 m

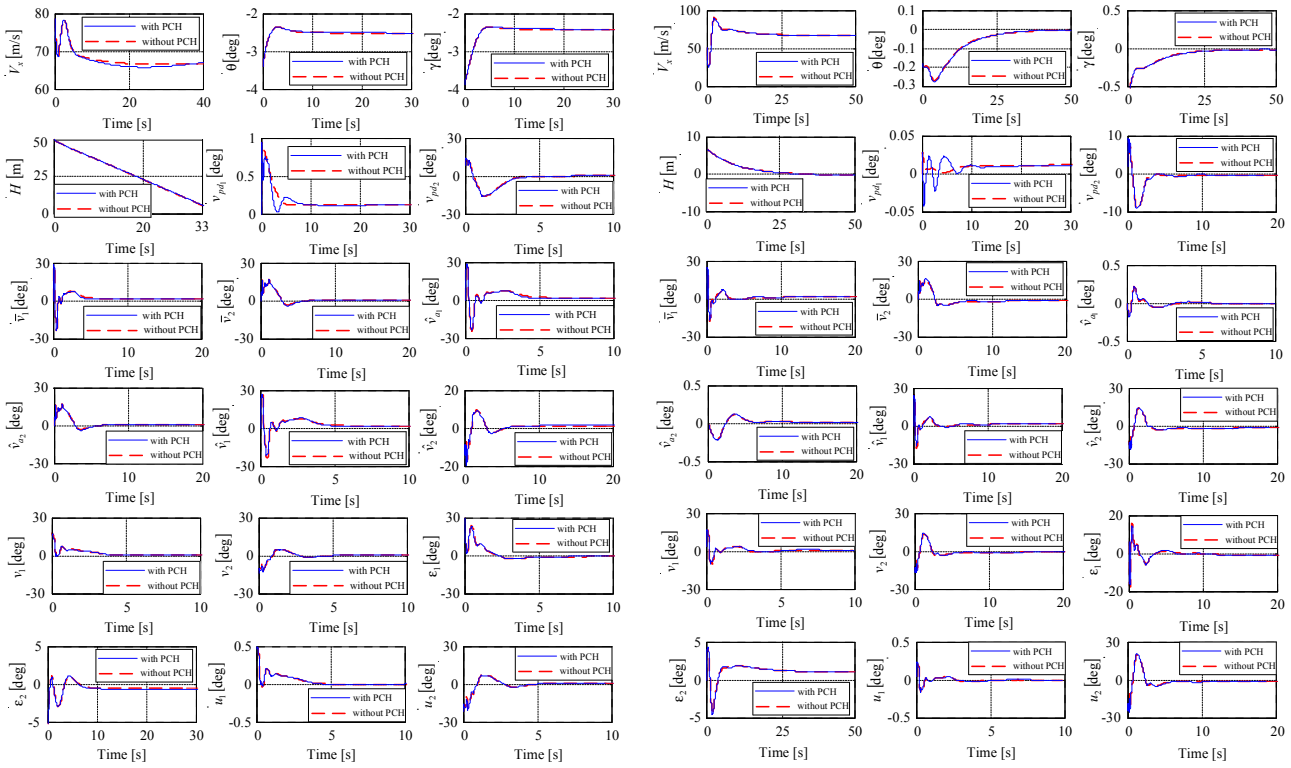

a. Glide slope **b. Flare**

Fig. 5. Dynamic characteristics for the new ALS (longitudinal plane)

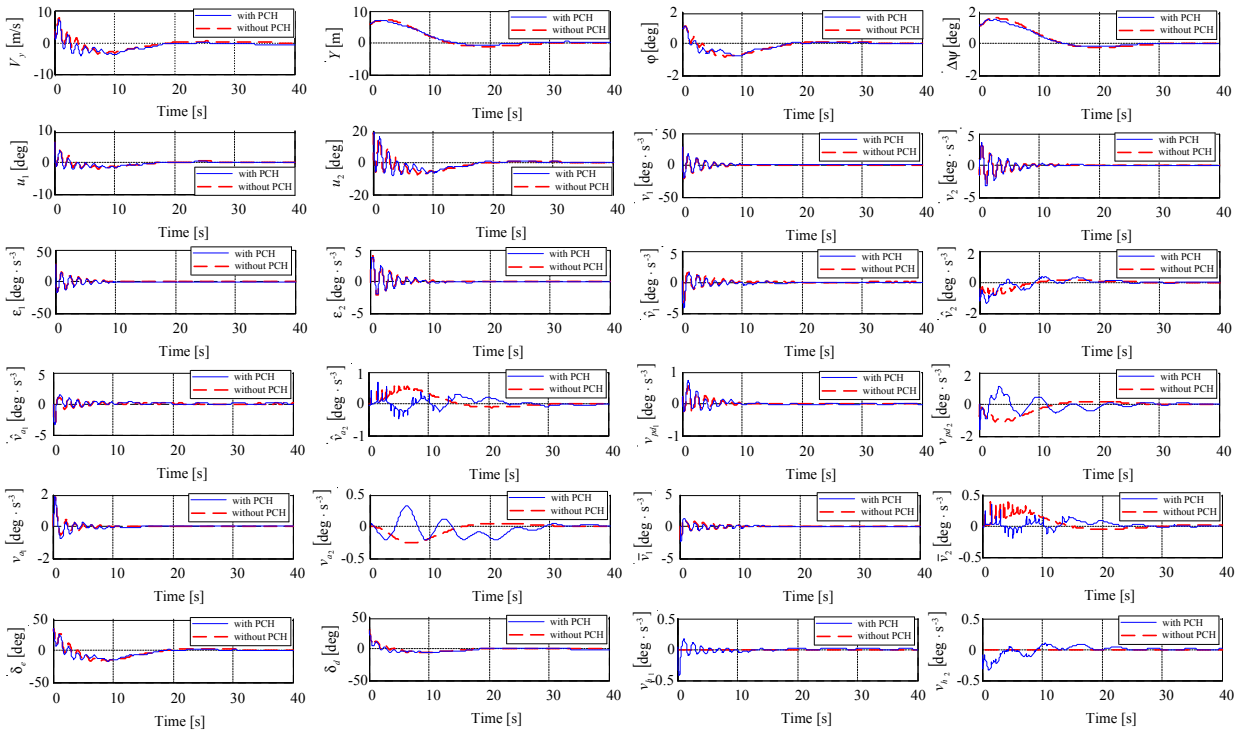

Fig. 6. Dynamic characteristics for the new ALS (lateral-directional plane)

for during flare. These errors meet the FAA (Federal Aviation Administration) accuracy requirements for best category (Category III) [13]; for longitudinal plane, the Category III's accuracy requirements involve altitude error less than 0.5 m (glide slope) and 0 m (flare), while, for lateral-directional plane, lateral deviation Y must be less than 4.1 m. For lateral plane, one also remarks that the subsystem responds very well and the cancelling of the airplane's lateral deviation with respect to runway $(Y \to 0)$.

V. Conclusion

The aim of this paper was the design of a complete ALS (longitudinal and lateral-directional planes) by using the neural networks and dynamic inversion based control techniques; two subsystems have been designed, software implemented, and validated; the former is used to control the landing process in longitudinal plane (glide slope and flare), while the latter is the lateral plane (initial approach) intended. The subsystems have been designed separately and put together to form a single ALS. The complete ALS has been software implemented, tested, and validated through numerical simulations; promising results have been obtained.

Acknowledgment

This work is supported by grant no. 89/1.10.2015 of the Romanian National Authority for Scientific Research and Innovation, CNCS-UEFISCDI, code PN-II-RU-TE-2014-4-0849.

References

[1] M. Lungu and R. Lungu, "Landing Auto-pilots for Airplane Motion in Longitudinal Plane using Adaptive Control Laws Based on Neural Networks and Dynamic Inversion," Asian Journal of Control, vol. 19, no. 1, pp. 1-15, 2017, DOI: 10.1002/asjc.1380, ISSN: 1561-8625.

[2] H. Vo and S. Sridhar, "Robust Control of F-16 Lateral Dynamics," Int. Journal of Aerospace and Mechanical Engineering, 2008.

[3] M. Lungu and R. Lungu, "Automatic Control of Airplane Lateral-directional Motion during Landing using Neural Networks and Radio-technical Subsystems," Neurocomputing Journal, vol. 171, pp. 471-481, 2016.

[4] R. Mori and S. Suzuki, "Neural Network Modeling of Lateral Pilot Landing Control," Journal of Airplane, no. 46, pp. 1721-1726, 2009.

[5] A. Calise, E. Johnson, M. Johnson, and J. Corban, "Applications of adaptive neural networks control to unmanned aerial vehicles," Journal of Harbin Institute of Technology, vol. 38, no. 11, pp. 1865-1869, 2006.

[6] A. Calise, S. Lee, and M. Sharma, "Direct Adaptive Reconfigurable Control of a Tailless Fighter Airplane", Rev. American Institute of Aeronautics and Astronautics, Georgia, USA, 2000.

[7] B. Parkinson, M. O'Connor, and K. Fitzgibbon, "Airplane automatic approach and landing using GPS," Global Positioning System: Theory and Applications, vol. II, pp. 397-425, 1996.

[8] R. Lungu, M. Lungu, and L. Grigorie, "ALSs with conventional and fuzzy controllers considering wind shears and gyro errors," Journal of Aerospace Engineering, vol. 26, no. 4, pp. 794-813, 2012.

[9] A. Calise, N. Hovakymyan, and M. Idan, "Adaptive Output Feedback Control of Nonlinear Systems Using Neural Networks," Automatica, vol. 37, no. 8, pp. 1201-1211, 2001.

[10] M. Lungu, "Flight control systems (Sisteme de conducere a zborului)," Sitech Publisher, Craiova, 2008.

[11] K. Xu, G. Zhang, and Y. Xu, "Intelligent Landing Control System for Civil Aviation Airplane with Dual Fuzzy Neural Network," 8th International Conference on Fuzzy Systems and Knowledge Discovery, pp. 171-175, 2011.

[12] D. Chwa and J. Choi, "Adaptive Nonlinear Guidance Law Considering Control Loop Dynamics," IEEE Transactions on Aerospace and Electronic Systems, vol. 39, no. 4, pp. 1134-1143, 2003.

[13] R. Braff, J. Powell, and J. Dorfler, "Applications of GPS to air traffic control," GPS: Theory and Applications, vol. II, pp. 327-374, 1996.